Pharmaceutical Research, Vol. 26, No. 7, July 2009 (© 2009)
DOI: 10.1007/s11095-009-9889-z

Research Paper

Cytotoxicity of Paclitaxel Incorporated in PLGA Nanoparticles on Hypoxic Human Tumor Cells

Cheng Jin,[1] Ling Bai,[2] Hong Wu,[3] Wenjie Song,[1] Guozhen Guo,[4] and Kefeng Dou[1,5]

Received November 5, 2008; accepted April 2, 2009; published online April 21, 2009

Purpose. The aim of this work was to prepare paclitaxel-loaded PLGA nanoparticles and determine cytotoxicity of released paclitaxel for two hypoxic human tumor cell lines: breast carcinoma (MCF-7) and carcinoma cervicis (HeLa).
Methods. Poly(D,L-lactide-co-glycolide) (PLGA) nanoparticles containing paclitaxel were prepared by o/w emulsification-solvent evaporation method. Physicochemical characteristics of nanoparticles were studied. Cellular uptake of nanoparticles was evaluated by transmission electronic microscopy and fluorescence microscopy. Flow cytometry quantified the number of cells held in G_2/M phase. Cell viability was determined by the ability of single cell to form colonies. Biodistribution of nanoparticles in mice was evaluated by fluorescence microscopy.
Results. The nanoparticles were spherical with average diameter 318±5.1 nm. The encapsulation efficiency was 88.52%. The drug release profile *in vitro* exhibited a biphasic pattern. Cellular uptake was observed. Co-culture of tumor cells with paclitaxel-loaded nanoparticles demonstrated that released paclitaxel retained its bioactivity to block cells in G_2/M phase. Paclitaxel-loaded nanoparticles exhibited cytotoxic effect on both hypoxic MCF-7 and HeLa cells and its cytotoxicity was more significant than that of free paclitaxel. Fluorescent nanoparticles were mainly distributed to liver and spleen of mice.
Conclusions. Paclitaxel-loaded PLGA nanoparticles may be considered a promising drug delivery system to eradicate hypoxic tumor cells.

KEY WORDS: human tumor cells; hypoxia; nanomedicine; nanopharmaceutical engineering; paclitaxel.

INTRODUCTION

Overwhelming clinical and experimental data demonstrate that tumor hypoxia, i.e. low tissue oxygen concentration, is associated with poor treatment outcome as hypoxic cells are refractive to chemo- and radiotherapy (1–5). The amount of evidence points to hypoxia as a potent physiological stimulus that promotes tumor progression, driving genetic change and selecting for malignant phenotypes (3,4,6). Hypoxia is also known to be a prognostic indicator, as hypoxic human tumors are more biologically aggressive and are more likely to recur locally and metastasize. Consequently, an important goal for cancer research has been to develop treatment strategies that selectively target this resistant tumor cell population. However, the agents and methods tested to target hypoxic tumor cells have little success, the reasons are as following: (a) the administration of inadequate drug in order to limit patient toxicity (7); (b) inability of the agent to access hypoxic tissues due to vascular insufficiency or acute changes in blood flow (8,9); (c) drug hydrophilicity (10); and/or (d) inability to compete against high tumor thiol levels (11–13).

The unique vascular structural changes associated with the pathophysiology of a tumor may provide opportunities for the use of nanoscale delivery systems. The abnormal tumor vasculature breaks all of the rules of normal blood vessel construction (14,15). One manifestation of this abnormality is a leaky endothelium (16–20), which is largely attributable to endothelial cells of tumor vessels having loose interconnections and focal intercellular openings. The extravasations of intravenously administrated nanoparticles are restricted to sites where the endothelial barrier has an open fenestration, such as inflammatory tissues and tumors, because normal tissues have tight endothelial junctions (21). Tumors have openings between defective endothelial cells ranging in size from 100 to 1,000 nm, with the majority of the gaps being between 200 and 900 nm (16), which strongly suggests that nanoparticles would more selectively extravasate in a tumor.

Nanoparticles of biodegradable polymers are widely investigated for controlled and targeted delivery of various drugs. The advantages of such a formulation include the sustained drug action on the lesion, reduced systemic side

Cheng Jin and Ling Bai contributed equally to this work.

[1] Department of Hepatobiliary Surgery, Xijing Hospital, Fourth Military Medical University, Xi'an, 710032, China.
[2] Department of Clinical Laboratories, Xi'an Gaoxin Hospital, Xi'an, 710075, China.
[3] Department of Pharmacy, Fourth Military Medical University, Xi'an, 710032, China.
[4] Department of Radiation Medicine, Fourth Military Medical University, Xi'an, 710032, China.
[5] To whom correspondence should be addressed. (e-mail: kefengdou@tom.com)

effects, facilitated extravasation into the tumor, high capability to cross various physiological barriers as well as controlled and targeted delivery of the drug (22–24). PLGA is an excellent synthetic biodegradable copolymer, which has been widely applied to formulate hydrophobic as well as hydrophilic drugs due to its excellent biocompatibility and biodegradability (25).

Paclitaxel is a potent anticancer chemotherapeutic agent, originally derived from the bark of the Pacific yew tree (Taxus brevifolia) (26), that is widely used in the treatment of solid tumors, particularly of the breast and ovaries (27). Paclitaxel exerts its cytotoxic effects by inducing tubulin polymerization resulting in unstable microtubules, which interferes with mitotic spindle function and ultimately arrests cells in the G_2/M phase of mitosis (27). Tumor cells exposed to paclitaxel treatment, as a result, then undergo programmed cell death or apoptosis (28). Because paclitaxel has profound effects on the process of mitosis, rapidly dividing cells such as those in tumors and those in highly proliferative normal tissues (such as bone marrow and oral mucosa) are most frequently affected by exposure to paclitaxel. Due to its high hydrophobicity, an adjuvant such as Cremophor EL has to be used to prepare injection as its clinical dosage form. Unfortunately, Cremophor EL causes serious side-effects and leads to hypersensitivity reactions in many patients (29–32). Moreover, it has been reported that Cremophor EL is able to block cells at the G_1 phase of the cell cycle preventing them to enter G_2/M phases and thus hampering the therapeutic effect of paclitaxel (33–35).

Some studies on the use of nanoparticles as carriers for paclitaxel have been published (36–40). In the previous work, we reported the radiosensitizing effect of paclitaxel-loaded nanoparticles on hypoxic tumor cells (41–43). Nevertheless, to our knowledge there are no studies on the literature regarding the cytotoxicity of paclitaxel-loaded nanoparticles on hypoxic tumor cells.

To overcome this therapeutically refractive cell population, the main goal of this work was to prepare paclitaxel-loaded PLGA nanoparticles and determine cytotoxicity of paclitaxel released from nanoparticles on hypoxic tumor cells.

MATERIALS AND METHODS

Materials

Drugs and Chemicals

Paclitaxel of 99.8% purity was purchased from Xi'an Biosep Biotechnology (Shaanxi Province, China). PLGA (*L*/*G*= 50/50, Mw=25,000) was from Chengdu Institute of Organic Chemistry, Chinese Academy of Science (Sichuan Province, China). 1,6-Diphenyl-1,3,5-hexatriene (DPH), propidium iodide (PI) and polyvinyl alcohol (PVA, Mw=30,000–70,000) were from Sigma-Aldrich (St. Louis, MO, USA). Dichloromethane (DCM, analytical grade) was purchased from Tianjin Chemical Factory (Tianjin City, China).

Cells

MCF-7 and HeLa cells were kindly provided by Dr. JY Liu and cultured as monolayers in Dulbecco's modified Eagle's medium (DMEM) supplemented with 10% fetal bovine serum (FBS), penicillin and streptomycin in a humidified atmosphere of 95% air and 5% CO_2 at 37°C. The cells were subcultured twice weekly. For experiments, the cells were grown in glass culture flasks and used when in exponential growth phase.

Animals

Male BALB/c mice (20±2 g) were supplied by the Experimental Animal Center of Fourth Military Medical University (Xi'an city, China). The animal were acclimatized at a temperature of 25±2°C and a relative humidity of 70±5% under natural light/dark conditions for 1 week before dosing. The study protocol was approved by and performed in accordance with the Committee of the Use of Live Animals in Teaching and Research at the Fourth Military Medical University.

Methods

Preparation of Paclitaxel-Loaded Nanoparticles

The preparation of PLGA nanoparticles incorporating paclitaxel was based on oil in water (o/w) emulsification-solvent evaporation method. Five milligrams of paclitaxel was dissolved in 4 ml DCM containing 2.5% (*w*/*v*) of PLGA. The resulting organic phase was poured into 20 ml aqueous phase containing 1% (*w*/*v*) of PVA whilst stirred and sonicated. The resulting emulsion was placed on the magnetic stirrer plate and continuously stirred at room temperature to evaporate DCM for 6 h. The nanoparticles were collected by centrifugation and washed four times with distilled water. The nanoparticles were then lyophilized and stored at 4°C before further analysis. In the present study, radiation with ^{60}Co source was used for the sterilization of nanoparticles.

Preparation of Fluorescent Nanoparticles

Fluorescent nanoparticles were prepared adding 10 mg of DPH (0.25% (*w*/*v*) calculated on the whole microemulsion) as fluorescent marker to the internal phase of DCM containing 2.5% (*w*/*v*) of PLGA and maintaining the other components of the formulations fixed. The fluorescent nanoparticles were obtained as described above for drug-loaded nanoparticles.

Determination of Drug Content in the Nanoparticles

Five milligrams of paclitaxel-loaded nanoparticles were dissolved in 1 ml of DCM. Then 3 ml of the mixture of acetonitrile: water (50:50, *v*/*v*) was added and extracted. A nitrogen stream was introduced to evaporate the DCM and a clear solution was obtained. The mixture containing the drug was determined using high-performance liquid chromatography (HPLC). The HPLC assay (Agilent 1100 series, CA, USA) was performed on a reverse phase Zorbax® C_{18} column. The mobile phase was a mixture of acetonitrile: water (50:50, (*v*/*v*)) delivered at a flow rate of 1.0 ml/min. Paclitaxel was detected at 227 nm with a

variable wavelength detector (VWD). The calibration curve for the quantification for paclitaxel was linear over the range of standard concentration between 50 and 100,000 ng/ml with a correlation coefficient of $R^2=1.0$. Loading efficiency and encapsulation efficiency (EE) were calculated as following:

$$\text{Loading efficiency (\%)} = (\text{amount of drug in nanoparticles} / \text{amount of drug loaded nanoparticles}) \times 100$$

$$\text{Encapsulation efficiency (\%)} = (\text{amount of drug in nanoparticles} / \text{initial amount of drug}) \times 100$$

Morphology and Particle Size

Nanoparticle morphology was examined by scanning electron microscope (SEM) (JSM-6700F, JEOL, Japan). Nanoparticles were analysed for their size distribution using photon correlation spectroscopy technique in a particle size analyzer (Zetasizer Nano S, Malvern Instruments, UK).

In Vitro Release

The release rate of paclitaxel from nanoparticles was measured in phosphate buffer saline (PBS) medium (pH 7.4) by an HPLC assay in triplicate. Paclitaxel-loaded nanoparticles were suspended in 10 ml of PBS in screw capped tubes, then placed in an orbital shaker maintained at 37°C and shaken at 120 rpm. At predetermined time intervals, the tubes were taken out of the shaker and centrifuged at 3,000 rpm for 5 min. The supernatant was taken for analysis of paclitaxel concentration. The precipitated nanoparticles were resuspended in 10 ml of fresh buffer and placed back in the shaker. The supernatant was extracted with 1 ml of DCM. Other procedure and HPLC analysis were conducted as previously described.

Fluorescence Microscopy

The cellular uptake of nanoparticles was studied using fluorescence microscopy. MCF-7 and HeLa cells were grown on coverslips for 24 h in a six-well tissue culture plate at 37°C. The cells were then cultured for 24 h with the fluorescent nanoparticles at a concentration of 2 mg/ml employed in the experiment. After rinsing with PBS, the cells were fixed by 95% ethanol solution for 30 min. The nuclei of the cells were then stained using 5 μg/ml of PI for 8 min at 37°C. The stained coverslips were mounted on a glass slide and photographed using fluorescence microscope (TE2000-S, Nikon, Japan). DPH and PI show blue and orange, respectively.

Transmission Electronic Microscopy (TEM)

The cellular uptake of nanoparticles was further studied using TEM. MCF-7 and HeLa cells were plated at 1×10^5 cells per well in six-well tissue culture plates for 24 h. The cells were incubated with paclitaxel-loaded nanoparticles for 24 h. The cells were washed twice with PBS and harvested by trypsinization. The cells were centrifuged at 1,000 rpm for 10 min. At this point, special care was taken when removing the precipitated cells. The pellets of cells were fixed by 3% glutaraldehyde solution. Fixed cells were washed with PBS and dehydrated three times sequentially in a graded series of ethanol solutions (50%, 70%, 90%, 95% and 100%). The cells were then soaked overnight in a 1:1 ratio of 100% alcohol and embedding resin. The resin-embedded cells were placed in capsules and the capsules were placed in a Pelco UV-2 Cryo Chamber at 4°C for 48 h for polymerization of the resin by UV radiation. The polymerized blocks were sectioned and the ultrathin sections were prepared. The cellular uptake of nanoparticles was evaluated by transmission electronic microscope (JEM-2000EX, JEOL, Japan).

Flow Cytometry Study

MCF-7 and HeLa cells were plated at 1×10^6 cells per well in six-well tissue culture plates for 24 h. Then cells were incubated with blank nanoparticles, free paclitaxel (80 ng/ml) and paclitaxel-loaded nanoparticles (60.18 ng/ml paclitaxel released at 24 h) for 24 h. The cells were fixed according to the unary-color staining procedure. Briefly, the cells were mechanically removed from the tissue culture plates and centrifuged at 1,000 rpm for 5 min. The supernatant was aspirated and the pellet was resuspended in 1 ml of PBS. The suspension was mixed continually while 2 ml of cold ethanol was added. The cells were stored at 4°C. Before flow cytometric analysis, the cells were stained with PI as fluorescent marker. Flow cytometry analysis was performed using an ELITE ESP machine (Beckman-Coulter, USA). The experiment was repeated three times. All the data are presented as means plus or minus SD. Significance of differences between the groups were determined with the One-Way ANOVA (SPSS10.0 statistical software), with the level of significance set at $P<0.05$.

Cell Survival Assay

Cell viability was measured by the ability of single cell to form colonies *in vitro*. The MCF-7 and HeLa cells were plated at 500 cells per well in six-well tissue culture plates for 24 h. Then cells were incubated in hypoxic condition for 12, 24, 48, 72, and 120 h with paclitaxel-loaded nanoparticles (45.93, 60.18, 76.17, 89.60, and 110.65 ng/ml paclitaxel released at 12, 24, 48, 72, and 120 h, respectively), free paclitaxel (60 ng/ml), blank nanoparticles and nothing as a negative control. To obtain hypoxia, the incubator was flushed with 95%N_2 and 5%CO_2 for 12, 24, 48, 72, and 120 h. Following administration, the media with paclitaxel-loaded nanoparticles, free paclitaxel and blank nanoparticles were removed, the fresh media were added. The cells were allowed to grow under standard culture conditions for 10–14 days. After this time interval, macroscopic colonies were stained with Giemsa and were counted manually. The experiment was repeated three times.

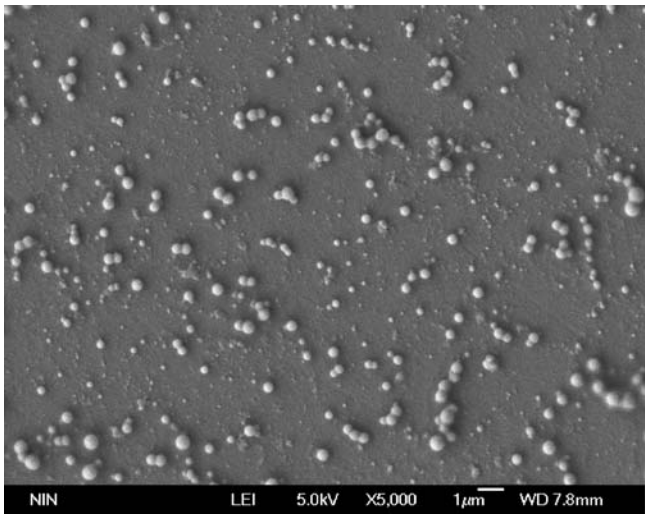

Fig. 1. Scanning electron microscopic photograph of paclitaxel-loaded nanoparticles.

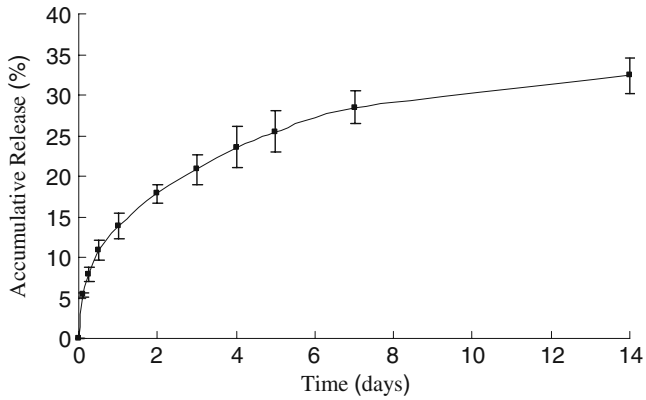

Fig. 3. The release profile of paclitaxel-loaded nanoparticles *in vitro*. The *error bars* indicate the standard deviation of the mean for $n=3$ independent experiments.

Biodistribution of Nanoparticles in Mice

Biodistribution of fluorescent nanoparticles in BALB/c mice ($n=5$) was evaluated by fluorescence microscope. For administration, nanoparticles were suspended in a certain volume of PBS (pH 7.4) in order to obtain the required concentration. The formulation was injected through the tail vein at the dose of 25 mg/kg mouse (1 mg/ml). After 2 h, the mice were killed by cervical dislocation and then tissues (brain, heart, lung, liver, kidney and spleen) were removed. Frozen sections were prepared immediately. The sections were placed at −20°C until further study. The sections were stained using 5 μg/ml of PI for 30 min at 37°C for the nuclei of the cells. The stained glass slides were mounted on the coverslips and photographed using fluorescence microscope (TE2000-S, Nikon, Japan).

RESULTS AND DISCUSSION

Characterization of Nanoparticle Delivery System

In order to increase therapeutic efficiency and reduce side effects, much effort has been devoted to optimization of the amount of drug incorporated into biodegradable polymeric particle delivery system. In this study, the drug EE and the loading efficiency for paclitaxel were 88.52% and 4.58%, respectively. Previous studies have reported similar high drug loading with paclitaxel in nanoparticles prepared with various polymers, such as poly(L-lactic acid) (PLLA), poly (ε-caprolactone) (PCL) and PLGA (36–40). The high EE of paclitaxel is due to its high partition coefficient and retention in the organic phase as the nanoparticles solidify.

Particle size plays an important role in determining the drug release behavior of the paclitaxel-loaded nanoparticles as well as their fate after administration. Smaller particles tended to accumulate in the tumor sites due to the facilitated extravasation (23) and a greater internalization was also observed (24). In addition, smaller particles make intravenous injection easier and their sterilization may be simply done by filtration (44,45). In the study, SEM showed that the nanoparticles were spherical in shape and had relatively smooth surface as shown in Fig. 1. The average diameter of the nanoparticles was 318±5.1 nm and the polydispersity index was 0.115 (Fig. 2).

In the release study, the release behaviour of paclitaxel from the polymer matrix exhibited a biphasic pattern characterised by a fast initial release during the first day (approximately 15%), followed by a slower and continuous release (Fig. 3). The amount of cumulated paclitaxel release over 14 days was about 30%. The initial release of drug could be explained by the release of some drug loosely bound on the surface of the nanoparticles by a mechanism of diffusion. This initial release was later followed by more controlled release for the 2-week study period. This drug release was a

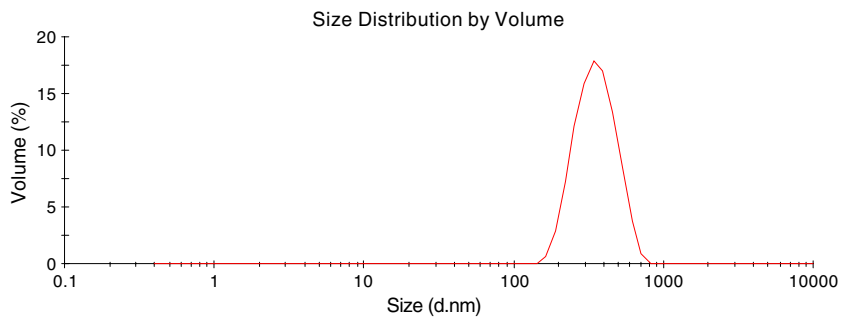

Fig. 2. Particle size distribution of paclitaxel-loaded nanoparticles.

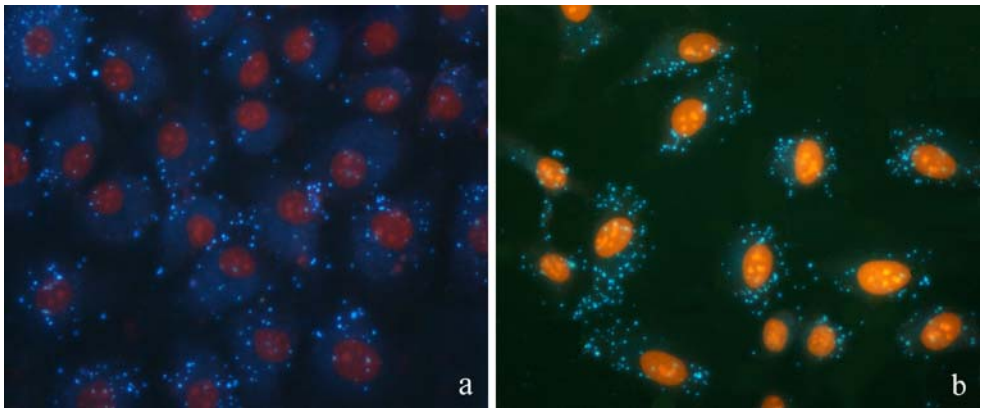

Fig. 4. Cellular uptake 24 h after incubation with fluorescent nanoparticles (**a** MCF-7 cells, **b** HeLa cells).

result of the degradation of the polymer. The release data demonstrated that the paclitaxel released from the nanoparticles increased with time. The results indicated that the drug release could be controlled. This ability is vital in the design of a degradable nanoparticle delivery system.

Evaluation of Paclitaxel-Loaded Nanoparticles Bioactivity

The cellular uptake of paclitaxel-loaded nanoparticles was determined by fluorescence microscopy. Fig. 4 showed the internalization of the nanoparticles in MCF-7 and HeLa cells following 24 h treatment. For the fluorescence observation, nanoparticles in the cells, as shown in Fig. 4, might not be due to those swallowed within cells but due to those located and adhered on the cells surface. In order to interpret these results, transmission electronic microscopy was further performed. Fig. 5 demonstrated that the tumor cells swallowed the drug-loaded nanoparticles. The bright blue spots in Fig. 4 were the fluorescent drug-loaded nanoparticles, but not the fluorescent dye that leaked from the nanoparticles and entered the cells, otherwise the fluorescence inside the cells was aequalis.

Flow cytometry was used to quantify the number of the two tumor cell lines held in the G_2/M phase of the cell cycle. The result was shown in Table I. The activity of the paclitaxel was expressed by the ability to block the tumor cells in G_2/M phase of the cell cycle. With the addition of free paclitaxel and paclitaxel-loaded nanoparticles to cells culture, the number of two tumor cell lines in the G_2/M phase significantly increased for MCF-7 and HeLa cells ($P<0.05$). The result demonstrated that active paclitaxel was released from the polymeric nanoparticles.

To understand the anti-tumor activity of paclitaxel, the hypoxic tumor cells cultured with blank nanoparticles, free paclitaxel and paclitaxel-loaded nanoparticles were determined using cell survival assay. The results of the bioactivity study were shown in Figs. 6 and 7. Plating efficiency was 85% and 58% for MCF-7 and HeLa cells, respectively. The treatments with free paclitaxel and paclitaxel-loaded nanoparticles resulted in an enhancement in the fraction of cell becoming clonogenically incompetent for both hypoxic MCF-

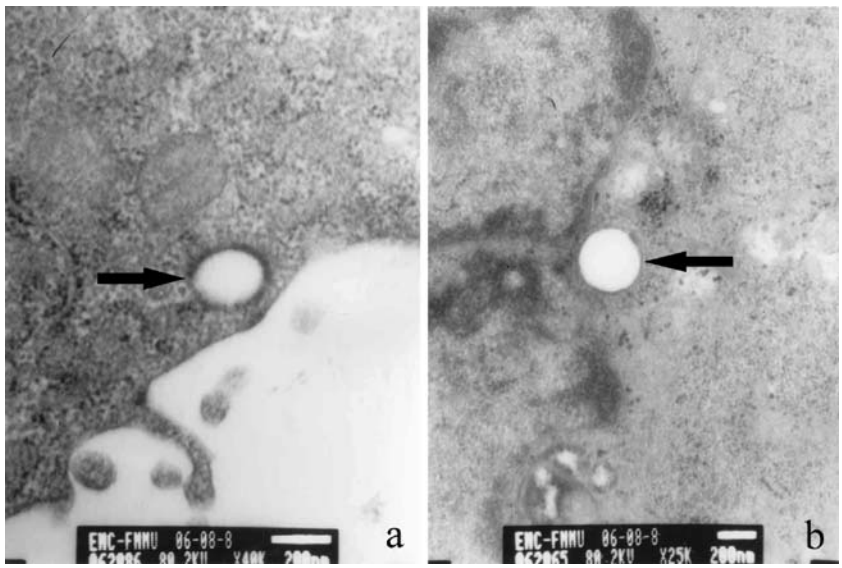

Fig. 5. Paclitaxel-loaded nanoparticles swallowed in MCF-7 and HeLa cells (**a**, **b**), respectively.

Table I. Flow Cytometry Result Showing the Cell Cycle Distribution of MCF-7 and HeLa Cells After 24 h of Exposure to Blank Nanoparticles, Free Paclitaxel and Paclitaxel-Loaded Nanoparticles

Cells	Treatment	Cell cycle (%)		
		G_1	S	G_2/M
MCF-7	Blank nanoparticles	76.8±4.4	19.7±2.7	3.5±1.2
	Free paclitaxel	55.6±3.9	24.9±4.8	20.5±3.3*
	Paclitaxel-loaded nanoparticles	63.5±5.9	22.1±4.6	14.4±3.1*
HeLa	Blank nanoparticles	68.6±7.4	25.8±3.7	5.6±2.0
	Free paclitaxel	54.4±5.3	20.3±3.9	25.3±4.7*
	Paclitaxel-loaded nanoparticles	59.9±4.5	23.4±3.8	16.7±2.1*

*$P<0.05$ (*vs* blank nanoparticles, $n=3$)

7 and HeLa cells. Their effects were enhanced with time. The therapeutic action of paclitaxel-loaded nanoparticles was more significant than that of free paclitaxel. The cell survival assay showed that bioactive paclitaxel was successfully released from the nanoparticle system. Due to the cytotoxicity of paclitaxel, the colony counts revealed that the colony numbers dropped with the addition of free paclitaxel and paclitaxel-loaded nanoparticles. According to the Figs. 6 and 7, the 50% effective concentrations (EC50) of paclitaxel released from the nanoparticles with time were obtained in 2.6 and 1.9 days for MCF-7 and HeLa cells, respectively. At these time points calculating according to the Fig. 3, the concentrations of paclitaxel were 85.03 and 74.22 ng/ml. The enhancement of paclitaxel activity mediated by its incorporation into nanoparticles can be explained by the fact that these systems can act as a reservoir for paclitaxel, protecting the drug from epimerization and hydrolysis (46,47) and providing not only a sustained release of paclitaxel but also contributing to the maintenance of its activity. In addition, it is reasonable to consider that cells become more prone to paclitaxel activity when the drug is delivered in the absence of Cremophor EL (which is the case for nanoparticles) since as reported above, this compound can antagonize paclitaxel activity (33–35). On the another hand, the higher sensitivity of the tumor cells to the drug-loaded nanoparticles than to the free drugs may be related to the marked uptake and accumulation of nanoparticles in the cells, where the drug-loaded nanoparticles should release the drugs, so enhancing their action. It is clear that the therapeutic effects of the drug-loaded nanoparticles would depend on internalization and sustained retention of nanoparticles by the diseased cells. Therefore, the mechanism of drug release from the nanoparticles is also of crucial importance for the extent of paclitaxel activity. In this regard, two distinct but not exclusive pathways can justify the enhancement of therapeutic activity of drug incorporated into nanoparticles: (I) nanoparticles can adsorb onto the cell membrane, leading to an increase in drug concentration near the cell surface, thus generating a concentration gradient that would favour a drug influx into the cell (48); (II) tumor cells can internalize polymeric nanoparticles allowing the drug to be released into the interior of the cells, thus contributing to an increase of the drug concentration near its site of action.

The distribution profiles of fluorescent drug-loaded nanoparticles in BALB/c mice 2 h after intravenous admin-

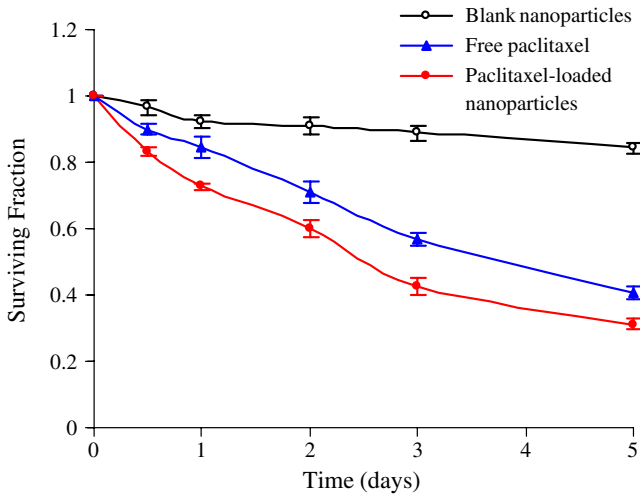

Fig. 6. Cytotoxicity of paclitaxel-loaded nanoparticles, free paclitaxel and blank nanoparticles in hypoxic MCF-7 cells. The *error bars* indicate the standard deviation of the mean for $n=3$ independent experiments.

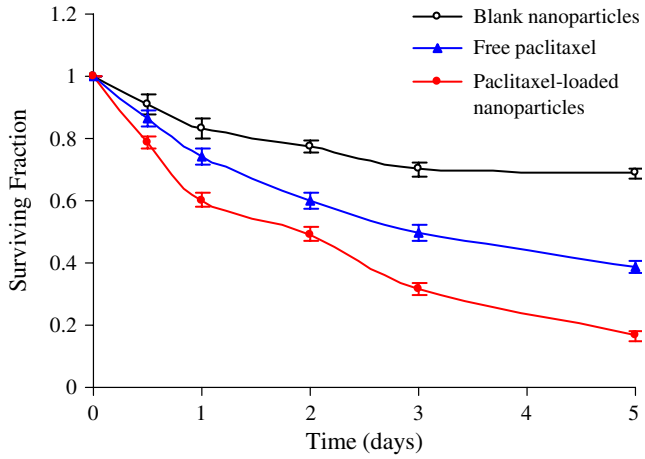

Fig. 7. Cytotoxicity of paclitaxel-loaded nanoparticles, free paclitaxel and blank nanoparticles in hypoxic HeLa cells. The *error bars* indicate the standard deviation of the mean for $n=3$ independent experiments.

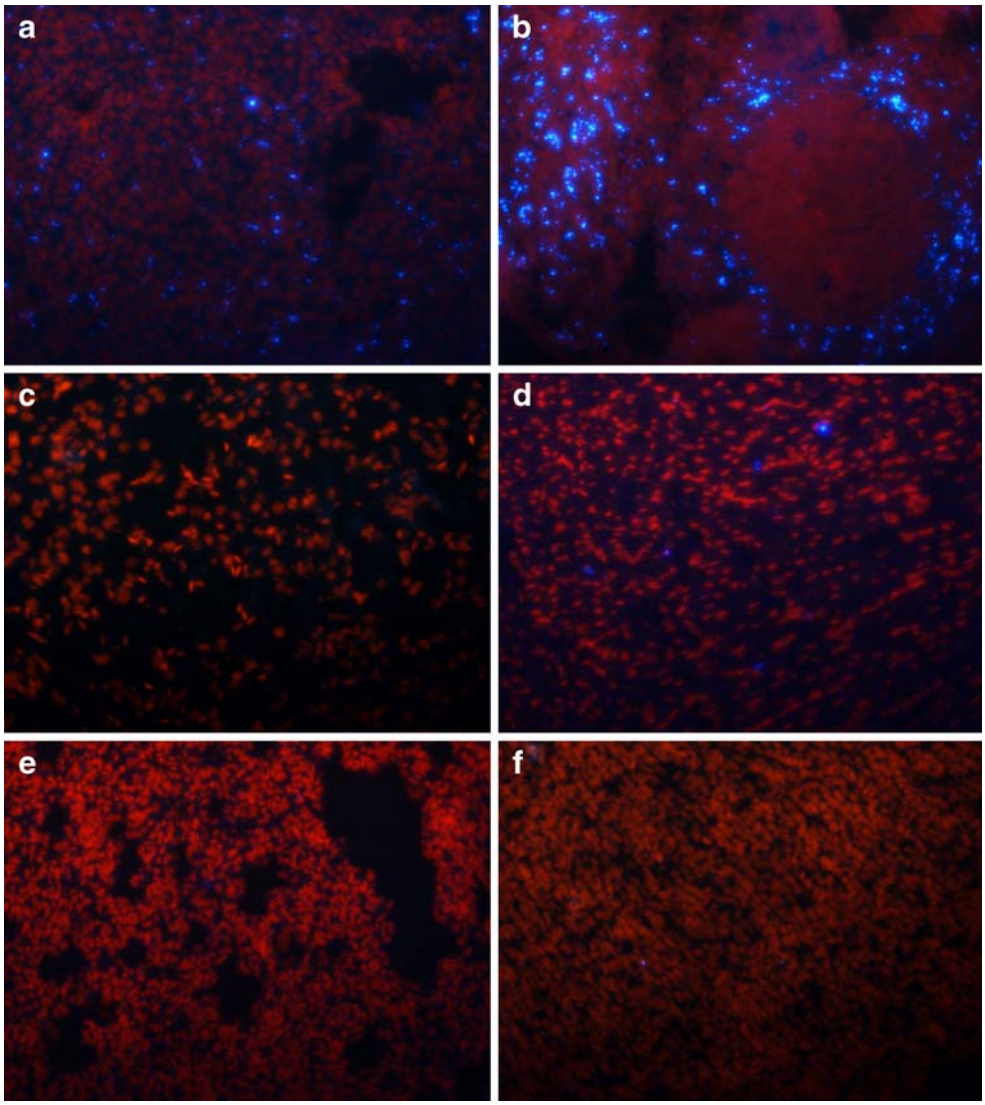

Fig. 8. The distribution profiles of fluorescent drug-loaded nanoparticles in BALB/c mice 2 h after intravenous administration (**a** liver, **b** spleen, **c** brain, **d** heart, **e** lung and **f** kidney).

istration were shown in Fig. 8. The nanoparticles were mainly distributed to the liver and spleen. The accumulation in brain, heart, lung and kidney of nanoparticles was very low or invisible. In concordance with previous studies, most particulate delivery systems are eliminated by the reticuloendothelial system (RES) within minutes, irrespective of their chemical composition, after intravenous injection. These particles accumulate in the liver and spleen following phagocytosis. For targeting to non-RES targets, such as tumor cells, avoidance of recognition by the RES is considered to be a major obstacle. In order to solve the problem, the further study on the drug-loaded nanoparticles specially targeting the tumor cells is significant and necessary. The rational approach is to conjugate therapeutic nanoparticles with monoclonal antibodies (mAbs) or other ligands that selectively bind to antigens or receptors that are usually abundantly or uniquely expressed on the tumor cell surface. These conjugated agents have demonstrated promising efficacy compared with conventional chemotherapy drugs in preclinical and clinical trials (49). In our further work, several ligand-targeted therapeutic strategies, using folate and transferrin, are studied.

CONCLUSIONS

These results obtained showed the release of bioactive paclitaxel from a degradable PLGA nanoparticle delivery system in a controlled manner. The cellular uptake of paclitaxel-loaded nanoparticles was observed. The presence of paclitaxel was found to significantly lower colony counts of hypoxic tumor cells. Moreover, it was shown that incorporation of paclitaxel in the PLGA nanoparticles significantly enhances its therapeutic action as compared to the free drug. Based on these results, it can be concluded that the formulations developed in this work may be considered promising systems for paclitaxel to eradicate hypoxic tumor cells.

ACKNOWLEDGEMENTS

This work was supported by a grant of National Nature Science Foundations of China: No30571828. The authors would like to thank Dr. JY Liu (Department of Radiation Medicine, Fourth Military Medical University) and Dr. ZH Teng (Department of Pharmacology, Fourth Military Medical University) for technical assistance.

REFERENCES

1. Gatenby RA, Kessler HB, Rosenblum JS, Coia LR, Moldofsky PJ, Hartz WH, Broder GJ. Oxygen distribution in squamous cell carcinoma metastases and its relationship to outcome of radiation therapy. Int J Radiat Oncol Biol Phys 1988;14:831–8.
2. Okunieff P, Hoeckel M, Dunphy EP, Schlenger K, Knoop C, Vaupel P. Oxygen tension distributions are sufficient to explain the local response of human breast tumors treated with radiation alone. Int J Radiat Oncol Biol Phys 1993;26:631–6.
3. Teicher BA. Hypoxia and drug resistance. Cancer Metast Rev 1994;13:39–68. doi:10.1007/BF00689633.
4. Hockel M, Schlenger K, Aral B, Mitze M, Schaffer U, Vaupel P. Association between tumor hypoxia and malignant progression in advanced cancer of the uterine cervix. Cancer Res 1996;56:4509–15.
5. Brizel DM, Sibley GS, Prosnitz LR, Scher RL, Dewhirst MW. Tumor hypoxia adversely affects the prognosis of carcinoma of the head and neck. Int J Radiat Oncol Biol Phys 1997;38:285–9. doi:10.1016/S0360-3016(97)00101-6.
6. Graeber TG, Osmanian C, Jacks T, Housman DE, Koch CJ, Lowe SW, Giaccia AJ. Hypoxia-mediated selection of cells with diminished apoptotic potential in solid tumours. Nature 1996;379:88–91. doi:10.1038/379088a0.
7. Urtasun RC, Coleman CN, Wasserman TH, Phillips TL. Clinical trials with hypoxic cell sensitizers: time to retrench or time to push forward? Int J Radiat Oncol Biol Phys 1984;10:1691–6.
8. Lesniak MS, Langer R, Brem H. Drug delivery to tumors of the central nervous system. Curr Neurol Neurosci Rep 2001;1:210–6. doi:10.1007/s11910-001-0020-z.
9. Jain RK. Vascular and interstitial barriers to delivery of therapeutic agents in tumors. Cancer Metast Rev 1990;9:253–66. doi:10.1007/BF00046364.
10. Brown DM, Gonsalez-Mendez R, Brown JM. Factors influencing intracellular uptake and radiosensitization by 2-nitroimidazoles *in vitro*. Radiat Res 1983;93:492–505. doi:10.2307/3576028.
11. Horan AD, Koch CJ. The K(m) for radiosensitization of human tumor cells by oxygen is much greater than 3 mmHg and is further increased by elevated levels of cysteine. Radiat Res 2001;156:388–98. doi:10.1667/0033-7587(2001)156[0388:TKMFRO]2.0.CO;2.
12. Koch CJ, Evans SM. Cysteine concentrations in rodent tumors: unexpectedly high values may cause therapy resistance. Int J Cancer 1996;67:661–7. doi:10.1002/(SICI)1097-0215(19960904)67:5<661::AID-IJC12>3.0.CO;2-8.
13. Koch CJ, Skov KA. Enhanced radiation-sensitivity by preincubation with nitroimidazoles: effect of glutathione depletion. Int J Radiat Oncol Biol Phys 1994;29:345–9.
14. Duncan R. The dawning era of polymer therapeutics. Nat Rev Drug Discov 2003;2:347–60. doi:10.1038/nrd1088.
15. Miller JC, Pien HH, Sahani D, Sorensen AG, Thrall JH. Imaging angiogenesis: applications and potential for drug development. J Natl Cancer Inst 2005;97:172–87.
16. Carmeliet P, Jain RK. Angiogenesis in cancer and other diseases. Nature 2000;407:249–57. doi:10.1038/35025220.
17. Hobbs SK, Monsky WL, Yuan F, Roberts WG, Griffith L, Torchilin VP, Jain RK. Regulation of transport pathways in tumor vessels: role of tumor type and microenvironment. Proc Natl Acad Sci U S A 1998;95:4607–12. doi:10.1073/pnas.95.8.4607.
18. Monsky WL, Fukumura D, Gohongi T, Ancukiewcz M, Weich HA, Torchilin VP, *et al.* Augmentation of tranvascular transport of macromolecules and nanoparticles in tumors using vascular endothelial growth factors. Cancer Res 1999;59:4129–35.
19. Hashizume H, Baluk P, Morikawa S, McLean JW, Thurston G, Roberge S, Jain RK, McDonald DM. Openings between defective endothelial cells explain tumor vessel leakiness. Am J Pathol 2000;156:1363–80.
20. McDonald DM, Baluk P. Significance of blood vessel leakiness in cancer. Cancer Res 2002;62:5381–5.
21. McDonald DM, Choyke PL. Imaging of angiogenesis: from microscope to clinic. Nat Med 2003;9:713–25. doi:10.1038/nm0603-713.
22. Brigger I, Dubernet C, Couvreur P. Nanoparticles in cancer therapy and diagnosis. Adv Drug Deliv Rev 2002;54:631–51. doi:10.1016/S0169-409X(02)00044-3.
23. Yuan F, Leuning M, Huang SK, Berk DA, Papahadjopoulos D, Jain RK. Microvascular permeability and interstitial penetration of sterically stabilized (stealth) liposomes in human tumor xenograft. Cancer Res 1994;54:3352–6.
24. Desai MP, Labhasetwar V, Walter E, Levy RJ, Amidon GL. The mechanism of uptake of biodegradable microparticles in CaCO-2 cells is size dependant. Pharm Res 1997;14:1568–73. doi:10.1023/A:1012126301290.
25. Jain RA. The manufacturing techniques of various drug loaded biodegradable poly(lactide-co-glycolide) (PLGA) devices. Biomaterials 2000;21:2475–90. doi:10.1016/S0142-9612(00)00115-0.
26. Adams JD, Flora KP, Goldspiel BR, Wilson JW, Arbuck SG, Finley R. Taxol: a history of pharmaceutical development and current pharmaceutical concerns. J Natl Cancer Inst Monogr 1993;15:141–7.
27. Costa MA, Simon DI. Molecular basis of restenosis and drug-eluting stents. Circulation 2005;111:2257–73. doi:10.1161/01.CIR.0000163587.36485.A7.
28. Pennati M, Campbell AJ, Curto M, Binda M, Cheng Y, Wang LZ, Curtin N, Golding BT, Griffin RJ, Hardcastle IR, Henderson A, Zaffaroni N, Newell DR. Potentiation of paclitaxel-induced apoptosis by the novel cyclin-dependent kinase inhibitor NU6140: a possible role for survivin downregulation. Mol Cancer Ther 2005;4:1328–37. doi:10.1158/1535-7163.MCT-05-0022.
29. Panchagnula R. Pharmaceutical aspects of paclitaxel. Int J Pharm 1998;172:1–15. doi:10.1016/S0378-5173(98)00188-4.
30. Arbuck SG. Taxol (paclitaxel): future directions. Ann Oncol 1994;6:S59–S62.
31. Dhanikula AB, Panchagnula R. Localized paclitaxel delivery. Int J Pharm 1999;183:85–100. doi:10.1016/S0378-5173(99)00087-3.
32. Singla AK, Garg A, Aggarwal D. Paclitaxel and its formulations. Int J Pharm 2002;235:179–92. doi:10.1016/S0378-5173(01)00986-3.
33. Liebmann J, Cook JA, Lipschultz C, Teague D, Fisher J, Mitchell JB. Cytotoxic studies of paclitaxel (Taxol®) in human tumor cell lines. Br J Cancer 1993;68:1104–9.
34. Liebmann J, Cook JA, Mitchell JB. Cremophor EL solvent for paclitaxel and toxicity. Lancet 1993;342:1428. doi:10.1016/0140-6736(93)92789-V.
35. Liebmann J, Cook JA, Lipschultz C, Teague D, Fisher J, Mitchell JB. The influence of Cremophor EL on the cell cycle effects of paclitaxel (Taxol) in human tumor cell lines. Cancer Chemother Pharmacol 1994;33:331–9. doi:10.1007/BF00685909.
36. Fonseca C, Simoes S, Gaspar R. Paclitaxel-loaded PLGA nanoparticles: preparation, physicochemical characterization and *in vitro* anti-tumoral activity. J Control Release 2002;83:273–86. doi:10.1016/S0168-3659(02)00212-2.
37. Mu L, Feng SS. PLGA/TPGS nanoparticles for controlled release of paclitaxel: effects of the emulsifier and the drug loading ratio. Pharmacol Res 2003;20:1864–72. doi:10.1023/B:PHAM.0000003387.15428.42.
38. Feng SS, Mu L, Win KY, Huang GF. Nanoparticles of biodegradable polymers for clinical administration of paclitaxel. Curr Med Chem 2004;11:413–24. doi:10.2174/0929867043455909.
39. Khin YW, Feng SS. *In vitro* and *in vivo* studies on vitamin E TPGS-emulsified poly(D,L-lactic-co-glycolic acid) nanoparticles for clinical administration of paclitaxel. Biomaterials 2006;27:2285–91. doi:10.1016/j.biomaterials.2005.11.008.
40. Liggins RT, Amours SD, Dematrick JS, Machan LS, Burt HM. Paclitaxel loaded poly(l-lactic acid) microspheres for the preven-

tion of intraperitonial carcinomatosis after a surgical repair and tumor cell spill. Biomaterials 2000;21:1959–69. doi:10.1016/S0142-9612(00)00080-6.
41. Jin C, Wu H, Liu J, Bai L, Guo G. The effect of paclitaxel-loaded nanoparticles with radiation on hypoxic MCF-7 cells. J Clin Pharm Ther 2007;32:41–7. doi:10.1111/j.1365-2710.2007.00796.x.
42. Jin C, Bai L, Wu H, Tian F, Guo G. Radiosensitization of paclitaxel, etanidazole and paclitaxel+etanidazole nanoparticles on hypoxic human tumor cells *In vitro*. Biomaterials 2007;28:3724–30. doi:10.1016/j.biomaterials.2007.04.032.
43. Jin C, Bai L, Wu H, Liu J, Guo G, Chen J. Paclitaxel-loaded poly (D,L-lactide-co-glycolide) nanoparticles for radiotherapy in hypoxic human tumor cells *In vitro*. Cancer Biol Ther 2008;7:911–6. doi:10.1158/1535-7163.MCT-07-0042.
44. Kwon GS, Kataoka K. Block copolymer micelles as long-circulating drug vehicles. Adv Drug Deliver Rev 1995;16:295–309. doi:10.1016/0169-409X(95)00031-2.
45. Konan YN, Gurney R, Allemann E. Preparation and characterization of sterile and freeze-dried sub-200 nm nanoparticles. Int J Pharm 2002;233:239–52. doi:10.1016/S0378-5173(01)00944-9.
46. Slichenmyer WJ, Von Hoff DD. Taxol: a new and effective anticancer drug. Anti-Cancer Drug 1991;2:519–30.
47. Dordunoo SK, Burt HM. Solubility and stability of taxol: effects of buffers and cyclodextrins. Int J Pharm 1996;133:191–201. doi:10.1016/0378-5173(96)04443-2.
48. Nemati F, Dubernet C, Colin de Verdiere A, Poupon MF, Treupel-Acar L, Puisieux F, Couvreur P. Some parameters influencing cytotoxicity of free doxorubicin and doxorubicin loaded nanoparticles in sensitive and multidrug resistant leukemic murine cells: incubation time, number of nanoparticles per cell. Int J Pharm 1994;102:55–62. doi:10.1016/0378-5173(94)90039-6.
49. Sapra P, Tyagi P, Allen TM. Ligand-targeted liposomes for cancer treatment. Curr Drug Deliv 2005;2:369–81. doi:10.2174/156720105774370159.